Program Digest, 2019 IEEE International Ultrasonics Symposium (IUS)
Glasgow, Scotland, October 6-9, 2019

Recent Developments in Adaptive Beamforming

Hideyuki Hasegawa
Graduate School of Science and Engineering, University of Toyama, Toyama 930-8555, Japan
hasegawa@eng.u-toyama.ac.jp

***Abstract*—Beamforming is an indispensable process to obtain an ultrasound image. In most of clinical ultrasound systems, the delay-and-sum (DAS) beamformer is implemented. The DAS beamformer applies time delays to ultrasonic echo signals received by individual transducer elements in an ultrasonic probe so that the phases of echoes from a point at the focus are aligned and, then, the delay compensated signals are summed to enhance the echo signal from the focal point. The DAS beamformer is very computationally efficient and suitable for real-time processing. On the other hand, its ability in suppression of off-axis signals is limited. To improve the performance of ultrasound beamformers, various studies on adaptive beamformers have been conducted for a long time and still being continuing nowadays. This paper provides a brief review on adaptive beamformers, particularly on the coherence-based adaptive imaging and its relation to the minimum variance beamforming.**

***Index Terms*—adaptive beamforming, coherence, minimum variance, noise estimate**

I. Introduction

Ultrasound beamforming methods are required to create a directivity in a transmit ultrasonic field. However, receive beamforming is particularly focused when we discussed adaptive beamformers, and we also focused on receive beamforming in this paper. In most of clinical ultrasound scanners, the delay-and-sum (DAS) beamforming is used. Ultrasound beamformers are required to extract echoes from every spatial point in an imaging field of view and construct an ultrasound image. The DAS beamformer applies time delays to ultrasonic echo signals received by individual transducer elements in an ultrasonic probe so that the phases of echoes from a point at the focus are aligned. The delay-compensated element echo signals are summed to obtain the output of the beamformer. The DAS beamformer is very computationally efficient and suitable for real-time processing. On the other hand, its ability in suppression of off-axis signals is limited.

For improvement of the performance of ultrasonic beamformers, various adaptive imaging methods have been developed. Hollman *et al.* introduced the coherence factor (CF), which had been developed previously [2], in medical ultrasound imaging to investigate effects of phase aberrations and evaluate ultrasound image quality [1]. In [1], CF was defined as the ratio of the coherent sum to the incoherent sum of the delay-compensated element echo signals. Figure 1 illustrates delay-compensated echo signals obtained from individual transducer elements. The phases of delay-compensated echo signals are aligned when the source of the echo (scatterer) is located at the focal point as illustrated in Fig. 1(a). In such a case, the coherent sum of the element echo signals across the array is high. Figure 1(b) illustrates the case when the source of the echo is not located at the focal point. In such a case, the phases of the element echo signals are not aligned and, as a result, the coherent sum of the element echo signals becomes low. The incoherent sum of the element echo signals corresponds to the total received energy, and CF, which is the ratio of the coherent sum to the incoherent sum, can evaluate focusing quality. The coherent sum of the element echo signals is also reduced by the phase aberration and, therefore, CF can evaluate effects of the phase aberration.

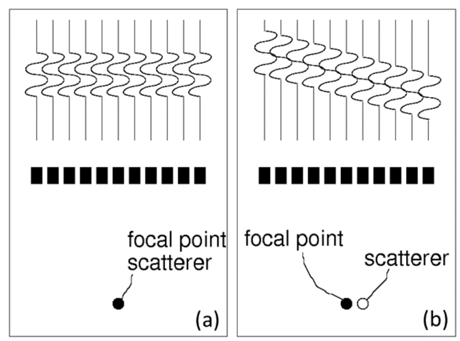

Fig. 1. Illustration of ultrasonic echo signals received by individual transducer elements in ultrasonic probe after delay compensation done by DAS beamformer. Locations of focal point and scatterer are coincident (a) and incoincident (b).

As described above, CF obtained from an off-axis echo signal is small. Based on such fundamental characteristics of CF, Li and Li later developed an adaptive imaging method, in which CF was used to weight outputs from a DAS beamformer to suppress a beamformed signal suffered from off-axis echo signals [3]. It was reported that the lateral resolution and contrast were improved by weighting the DAS beamformer output with CF.

The above-mentioned adaptive imaging method weights the output of the DAS beamformer with CF. On the other hand, Synnevåg *et al.* introduced the minimum variance (MV) beamformer [4], which had been developed previously by Capon [5], to determine beamforming weights to element echo signals adaptively. In DAS beamforming, a fixed beamforming weight, such as rectangular and Hanning apodization, is used. The MV beamformer determines the beamforming weights depending on received element echo signals and realizes significant improvements in lateral resolution.

In the adaptive determination of the beamforming weights, the noise covariance matrix needs to estimated, and it is an very important step in MV beamforming which determines quality of a resultant image. The covariance matrix is in general estimated from the received element echo signals. Needless to say, the received element echo signals contains a desired echo signal from a point at the focus. To suppress components which is coherent with the echo signal from a point at the focus, the spatial smoothing technique, namely, sub-array averaging, was introduced to obtain an estimate of the noise covariance matrix [4], [6]. Also, a constant value was added to the diagonal of the estimated covariance matrix to increase the robustness because the inversion of the covariance matrix is necessary to obtain the adaptive beamforming weights.

As described above, the estimation of noise, in this case, including off-axis components, electrical noise, etc. is very important in adaptive imaging. Although there are a number of new adaptive beamforming methods, including delay multiply and sum beamforming [9], pixel based beamforming [10], aberration correction [11], and deep-learning based beamforming [12], developed so far, this paper concentrates on the brief review of methods for estimation of noise in adaptive beamforming and their relation to coherence-based imaging, which is described in [8].

II. Principles

A. Coherence factor (CF)

Let us define a vector of ultrasonic echo signals received by individual transducer elements as follows:

$$\mathbf{s} = [s_0, s_1, s_2, ..., s_{M-1}],^{\mathrm{T}} \tag{1}$$

where M is the number of elements in an array, and $^{\mathrm{T}}$ denotes the transpose operation.

In the DAS beamforming, the beamformer output p_{DAS} is obtained as follows:

$$p_{\mathrm{DAS}} = \mathbf{w}^{\mathrm{H}} \cdot \mathbf{s}, \tag{2}$$

where $^{\mathrm{H}}$ denotes the conjugate transpose operation, and $\mathbf{w}$ is a beamforming weight vector expressed as follows:

$$\mathbf{w} = [w_0, w_1, w_2, ..., w_{M-1}]^{\mathrm{T}}. \tag{3}$$

In the present study, $s_m \quad (m = 0, 1, 2, ..., M-1)$ denotes delay-compensated element echo signals. In such a case, $\mathbf{w}$ becomes a vector of ones, which corresponds to rectangular apodization.

In [1], [3], CF is defined as follows:

$$CF = \frac{\left|\sum_{m=0}^{M-1} s_m\right|^2}{M \sum_{m=0}^{M-1} |s_m|^2}. \tag{4}$$

B. Minimum variance beamforming

From Eq. (2), the expected power of a beamformer output p_{BF} is obtained as follows:

$$\mathrm{E}\left[|p_{\mathrm{BF}}|^2\right] = \mathrm{E}\left[\mathbf{w}^{\mathrm{H}}\mathbf{s}^{\mathrm{H}}\mathbf{s}\mathbf{w}\right] = \mathbf{w}^{\mathrm{H}}\mathbf{R}\mathbf{w}, \tag{5}$$

where $\mathbf{R}$ is a covariance matrix.

The minimum variance beamformer estimates the beamformer weights $\mathbf{w}_{\mathrm{MV}}$ so that the variance of the beamformer output is minimized, while keeping echo signals from a direction of interest unaffected. This can be achieved as

$$\begin{aligned} \mathbf{w}_{\mathrm{MV}} &= \arg\min_{\mathbf{w}} \mathrm{E}\left[|\mathbf{w}\mathbf{s}|^2\right] \\ &= \arg\min_{\mathbf{w}} \mathbf{w}^{\mathrm{H}}\mathbf{R}\mathbf{w}, \quad \text{subject to } \mathbf{w}^{\mathrm{H}}\mathbf{a} = 1, \end{aligned} \tag{6}$$

where $\mathbf{a}$ is a steering vector and is a vector of ones when the time domain delay compensation is applied to element echo signals. The solution is obtained as follows:

$$\mathbf{w}_{\mathrm{MV}} = \frac{\mathbf{R}^{-1}\mathbf{a}}{\mathbf{a}^{\mathrm{H}}\mathbf{R}^{-1}\mathbf{a}} \tag{7}$$

C. Wiener beamforming

The Wiener beamformer estimates the beamforming weights in a minimum mean square error sense [8]. The optimization problem is expressed as follows:

$$\mathbf{w}_{\mathrm{wiener}} = \arg\min_{\mathbf{w}} \mathrm{E}\left[\left|p - \mathbf{w}^{\mathrm{H}}\mathbf{s}\right|^2\right]. \tag{8}$$

The solution to this problem is obtained as follows:

$$\mathbf{w}_{\mathrm{wiener}} = |p|^2\, \mathbf{R}^{-1}\mathbf{a}, \tag{9}$$

where p is the amplitude of an echo from the focal point.

Let us model the element echo signal as follows:

$$\mathbf{s} = p\mathbf{a} + \mathbf{n}, \tag{10}$$

where $\mathbf{n} = [n_0, n_1, n_2, ..., n_{M-1}]^{\mathrm{T}}$ is zero-mean random noise. In this case, Eq. (5) can be rewritten as follows [8]:

$$\mathbf{R} = |p|^2\, \mathbf{a}\mathbf{a}^{\mathrm{H}} + \mathbf{n}\mathbf{n}^{\mathrm{H}} = |p|^2\, \mathbf{a}\mathbf{a}^{\mathrm{H}} + \mathbf{R}_{\mathrm{n}}, \tag{11}$$

where $\mathbf{R}_{\mathrm{n}} = \mathbf{n}^{\mathrm{H}}\mathbf{n}$ is the noise covariance matrix.

Using the relation of Eq. (11), Eq. (9) can be rewriting as follows:

$$\mathbf{w}_{\mathrm{wiener}} = \frac{|p|^2}{|p|^2 + {\mathbf{w}_{\mathrm{MV}}}^{\mathrm{H}}\mathbf{R}_{\mathrm{n}}\mathbf{w}_{\mathrm{MV}}}\mathbf{w}_{\mathrm{MV}}. \tag{12}$$

By referring to Eq. (5), it is found that the second term in the denominator of Eq. (12) corresponds to the power of the residual noise in the output of the MV beamformer. Therefore, the output of the Wiener beamformer corresponds to the output of the MV beamformer multiplied by a scalar factor depending on the amplitude of a signal of interest and residual noise.

It was shown that the scaler parameter in Eq. (12), namely, Wiener postfilter, can be available for any distortionless beamformer, including the DAS beamformer [8]. The Wiener postfilter H_{wiener} can be obtained by solving a minimization problem as

$$H_{\mathrm{wiener}} = \arg\min_{\mathbf{w}} \mathrm{E}\left[\left|p - H\mathbf{w}^{\mathrm{H}}\mathbf{s}\right|^2\right]. \tag{13}$$

The solution to this problem is obtained as follows:

$$H_{\text{wiener}} = \frac{|p|^2}{\mathbf{w}^{\text{H}}\mathbf{R}\mathbf{w}} = \frac{|p|^2}{|p|^2 + \mathbf{w}\mathbf{R}_{\text{n}}\mathbf{w}}. \tag{14}$$

As shown in Eq. (5), the power of a beamformer output is $\mathbf{w}^{\text{H}}\mathbf{R}\mathbf{w} = |p|^2 + \mathbf{w}^{\text{H}}\mathbf{R}_{\text{n}}\mathbf{w}$. By multiplying a scaler factor of H_{wiener} in Eq. (14), the power of a beamformer output becomes $|p|^4 / \left(|p|^2 + \mathbf{w}^{\text{H}}\mathbf{R}_{\text{n}}\mathbf{w}\right)$, which is closer to the power $|p|^2$ of a signal of interest. The Wiener postfilter try to recover the distortion in the amplitude of a beamformer output, however, the scaler factor is multiplied to both a signal of interest and noise. Therefore, it does not change the signal-to-noise ratio of the beamformer output. It is a quite different nature of the Wiener postfilter from the MV beamformer.

D. Noise estimate in CF

The relation between the Wiener postfilter and CF is also shown in [8]. Since the DAS beamformer assumes noise contained in the received signal as white noise, CF in Eq. (4) is rewritten as follows:

$$\begin{aligned} CF &= \frac{\left|\sum_{m=0}^{M-1} s_m\right|^2}{\left|\sum_{m=0}^{M-1} s_m\right|^2 + \frac{1}{M}\sum_{m=0}^{M-1}\left|s_m - \frac{1}{M}\sum_{i=0}^{M-1} s_i\right|^2} \\ &= \frac{|p|^2}{|p|^2 + M\mathbf{w}^{\text{H}}\mathbf{R}_{\text{n}}\mathbf{w}}, \\ &\quad \text{for } \mathbf{R}_{\text{n}} = \sigma^2\mathbf{I} \text{ and } \mathbf{w} = \frac{1}{M}\mathbf{1}, \end{aligned} \tag{15}$$

where σ_{n}^2 and $\mathbf{I}$ are the power of noise and identity matrix, respectively, and $\mathbf{1}$ denotes a vector of ones.

From the comparison of Eq. (15) with Eq. (14), it is found that CF overestimates the output noise power by a factor of M. Therefore, CF causes excessive suppression of echo signals with noise. It is preferable to estimate the power of noise in a Wiener-postfilter sense.

E. Noise estimators

As described above, the estimation of noise is very important in adaptive imaging. A few methods for estimation of noise is presented in [8].

As described above, the output noise power is expressed as follows:

$$\text{E}\left[\left|\mathbf{w}^{\text{H}}\mathbf{n}\right|^2\right] = \mathbf{w}^{\text{H}}\mathbf{R}_{\text{n}}\mathbf{w}. \tag{16}$$

By assuming that an estimate of a signal of interest $\widehat{p}$ is obtained by DAS or MV beamformer, the residual noise is expressed by $(\mathbf{s} - \widehat{p}\mathbf{1})$. Therefore, the noise covariance matrix is estimated as follows:

$$\widehat{\mathbf{R}}_{\text{n}} = \frac{1}{K}\sum_{k=0}^{K-1}\left(\mathbf{s}_k - \widehat{p}\mathbf{1}\right)\left(\mathbf{s}_k - \widehat{p}\mathbf{1}\right)^{\text{H}}, \tag{17}$$

where $\mathbf{s}_k = [s_k, s_{k+1}, ..., s_{k+L-1}]$, and L denotes the number of elements in a sub-array. An averaging method taken in Eq. (17) is called the sub-array averaging, which is also used to obtain a robust estimate of the covariance matrix in Eq. (7).

Another method for estimation of the output noise power is realized by assuming white noise. Under such an assumption, the noise covariance matrix is expressed as follows:

$$\widehat{\mathbf{R}}_{\text{n}} = \frac{1}{M}\sum_{m=0}^{M-1}\left|s_m - \widehat{p}\right|^2\mathbf{I} = \widehat{\sigma}_{\text{n}}^2\mathbf{I}. \tag{18}$$

III. Experimental Results

In this section, the definitions of CF and Wiener postfilter are given by Eqs. (4) and (14). In the present study, the performances of those adaptive imaging methods were examined in plane-wave high-frame-rate ultrasound imaging. An ultrasonic probe at a center frequency of 7.5 MHz with 192 transducer elements at spacing of 0.1 mm was used. Ultrasonic echo signals received by individual transducer elements in the probe was acquired at a sampling frequency of 31.25 MHz. Each receiving beam was obtained with echo signals from 72 elements.

Figures 2(1) and 2(2) are ultrasonic images of strings embedded in tissue mimicking material and anechoic cyst phantom, respectively. Those images were obtained by DAS beamforming with CF (Fig. 2(a)) and Wiener postfilter (Fig. 2(b)). In the images of the strings, the lateral resolution, which is the lateral width at half maximum of an echo from the string, is improved from 0.32 mm to 0.24 mm using the Wiener postfilter. Also, the visibility of echoes from speckle generating material is also improved by the Wiener postfilter because the excessive suppression of echoes affected by interference is reduced in comparison with CF. On the other hand, the contrast ratio evaluated from the images of the cyst phantom was slightly decreased from -0.2 dB to -0.5 dB. The contrast-to-noise ratios (CNRs) obtained with CF and Wiener postfilter were -1.8 dB and -2.4 dB, respectively.

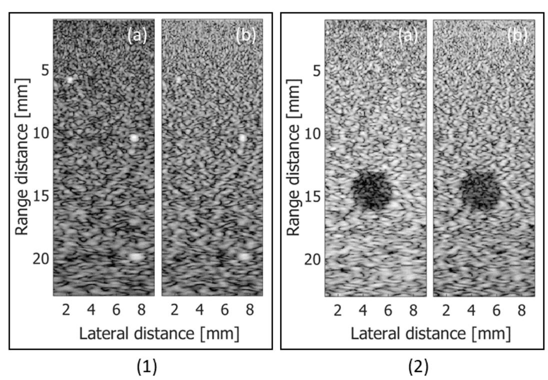

Fig. 2. B-mode images of string (1) and anechoic cyst (2) phantoms. Images are obtained by DAS beamforming with CF (a) and Wiener postfilter (b) and shown with dynamic range of 80 dB.

As described in Section II-C, the power of a beamformer output with the Wiener postfilter is $|p|^4 / \left(|p|^2 + \mathbf{w}^{\text{H}}\mathbf{R}_{\text{n}}\mathbf{w}\right)$.

In other words, a distorsionless amplitude estimate can be obtained with a scaling factor, which is the square root of the Wiener postfilter. Therefore, beamformer outputs multiplied by the square root of the Wiener postfilter was compared with the DAS beamformer, which is also one of the distorsionless beamformers. Figures 3(1) and 3(2) show B-mode images of strings embedded in tissue mimicking material and anechoic cyst phantom, respectively. Those images were obtained with DAS beamforming only (Fig. 3(a)) and DAS beamforming followed by weighting with the square root of the Wiener postfilter (Fig. 3(b)).

As can be seen in Fig. 3(1), the lateral resolution obtained with a scaling factor of the square root of the Wiener postfilter was 0.31 mm, which was significantly better than that obtained by the DAS beamforming of 0.54 mm. The lateral resolution obtained with the square root of the Wiener postfilter was still better than that obtained with CF.

The contrast ratios were evaluated from the images of the cyst phantom shown in Fig. 3(2). The contrast ratio obtained with a scaling factor of the square root of the Wiener postfilter was -1.3 dB, which was worse than that obtained with CF (-0.2 dB) but significantly better than that obtained by the DAS beamforming (-3.3 dB). The CNR obtained with a scaling factor of the square root of the Wiener postfilter was 0.2 dB, which was worse than that obtained by the DAS beamforming (4.1 dB) but significantly better than that obtained with CF (-1.8 dB).

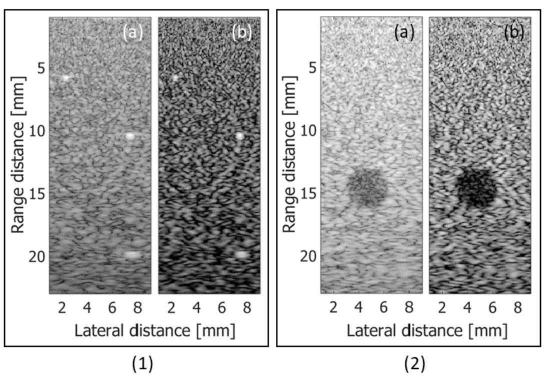

Fig. 3. B-mode images of string phantom (1) and anechoic cyst phantom (2). Images are obtained by DAS beamforming only (a) and DAS beamforming with square root of Wiener postfilter (b) and shown with dynamic range of 60 dB.

Figures 4(1) and 4(2) shows B-mode images of string and anechoic cyst phantoms, respectively. The images in Figs. 4(a) and 4(b) were obtained with CF and Wiener postfilter estimated with MV beamforming, respectively. The lateral resolutions, contrast ratios, and CNRs obtained with CF and Wiener postfilter were 0.12 mm and 0.17 mm, -1.7 dB and -0.1 dB, -7.7 dB and -8.6 dB, respectively.

IV. Conclusion

Recently, adaptive beamforming methods are intensively studied because programmable ultrasound scanners, which allow us to acquire ultrasonic echo signals received by individual transducer elements in an ultrasonic probe, are now widely available. As shown by the experimental results in this paper, adaptive beamformers improves resolution and contrast significantly, however, the performances are largely dependent on the methods for estimation of noise components. Furthermore, those improvements are realized at the expense of CNR. CNR is also an important metric determining the accuracy of medical diagnosis and is desired to be improved in future work.

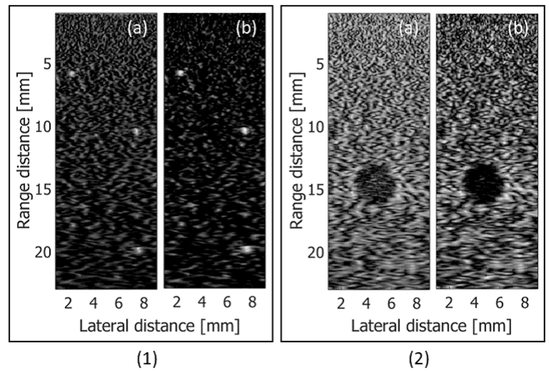

Fig. 4. B-mode images of string phantom (1) and anechoic cyst phantom (2). Images are obtained with CF (a) and Wiener postfilter (b) both estimated with MV beamforming. Images are shown with dynamic ranges of 80 dB.

References

[1] K. W. Hollmand, K. W. Rigby, and M. O 竇僖 onnell, "Coherence factor of speckle from a multi-row probe,"*in Proc. IEEE Ultrasonics Symp.*, 1999, pp. 1257–1260.

[2] R. Mallart and M. Fink, "Adaptive focusing in scattering media through sound-speed inhomogeneities: The van Cittert-Zernike approach and focusing criterion,"*J. Acoust. Soc. Am.*, vol. 96, no. 6, pp. 3721–3732, 1994.

[3] P.-C. Li and M.-L. Li, "Adaptive imaging using the generalized coherence factor,"*IEEE Trans. Ultrason. Ferroelectr. Freq. Control*, vol. 50, no. 2, pp. 128–141, 2003.

[4] J. F. Synnevåg, A. Austeng, and S. Holm, "Adaptive beamforming applied to medical ultrasound imaging,"*IEEE Trans. Ultrason. Ferroelectr. Freq. Control*, vol. 54, no. 8, pp. 1606–1613, 2007.

[5] J. Capon, "High-resolution frequency-wavenumber spectrum analysis,"*Proc. IEEE*, vol. 57, pp. 1408–1418, 1969.

[6] T.-J. Shan, M. Wax, and T. Kailath, "On spatial smoothing for direction-of-arrival estimation of coherent signals,"*IEEE Trans. Acoust. Speech Signal Process.*, vol. 33, no. 4, pp. 806–811, 1985.

[7] S.-L. Wang and P.-C. Li, "MVDR-Based coherence weighting for high-frame-rate adaptive imaging,"*IEEE Trans. Ultrason. Ferroelectr. Freq. Control*, vol. 56, no. 10, pp. 2097–2110, 2009.

[8] C.-I. C. Nilsen and S. Holm, "Wiener beamforming and the coherence factor in ultrasound imaging,"*IEEE Trans. Ultrason. Ferroelectr. Freq. Control*, vol. 57, no. 6, pp. 1329–1346, 2010.

[9] G. Matrone, A. S. Savoia, G. Caliano, and G. Magenes, "The delay multiply and sum beamforming algorithm in ultrasound B-mode medical imaging,"*IEEE Trans. Med. Imaging*, vol. 34, no. 4, pp. 940–949, 2015.

[10] N. Q. Nguyen and R. W. Prager, "High-resolution ultrasound imaging with unified pixel-based beamforming,"*IEEE Trans. Med. Imaging*, vol. 35, no. 1, pp. 98–108, 2016.

[11] A. Aubry and A. Derode, "Detection and imaging in a random medium: A matrix method to overcome multiple scattering and aberration,"*J. Appl. Phys.*, vol. 106, pp. 044903, 2009.

[12] A. Luchies and B. Byram, "Deep neural networks for ultrasound beamforming,"*2017 IEEE International Ultrason. Symp.*, 2017. DOI: 10.1109/ULTSYM.2017.8092159